

Detection of Electrical Fault in Medium Voltage Installation Using Support Vector Machine and Artificial Neural Network

Yazid Laib Dit Leksir^{a,b,*}, Kadour Guerfi^c, Ammar Amouri^d, and Abdelkrim Moussaoui^a

^a *Laboratoire de Génie Electrique de Guelma, Université 8 May 1945, Guelma, Algérie*

^b *Institut d'électronique, Université constantine1, Constantine, 25000 Algérie*

^c *Centre de recherche en technologie industrielle, CRTI, Chéraga, Algérie*

^d *Department of Mechanical Engineering, Freres Mentouri University, Constantine, Algeria*

*e-mail: yaziddl@yahoo.fr

Received September 26, 2021; revised February 25, 2022; accepted March 1, 2022

Abstract—Infrared thermography plays an important role in the inspection of electrical installations allowing to avoid failures and breakdowns. Condition monitoring using thermal imaging techniques can be effectively achieved by keeping a safe distance from the inspected equipment. The major advantage when using these techniques is that it is not mandatory to stop the equipment during the inspection. Moreover, and since data collection is done without contact, dangerous interventions can be avoided. Any irregular areas of the compound being checked will be reflected as abnormal areas. This work aims to visualize the anomalies existing in electric equipment during inspections of many installations by means of the A40M thermo-vision imager. The segmentation results show that the binarization accuracy of the supervised SVM classifier is better than that of the supervised ANN algorithm, and it applies to both larger and smaller faults. However, the application of artificial neural networks requires more calculation time due to training and testing for verification of the region of interest. Comparison between the thermal images obtained using both methods is discussed.

Keywords: thermal vision, fault diagnostics, condition monitoring, binarization methods

DOI: 10.1134/S1061830922030081

INTRODUCTION

Safety and stability of electrical equipment play a very important part in guaranteeing the cost-effective operation and prosperity of industrial plants. Nowadays, evaluating the performance and protection of electrical installations relies on visual inspection, and with the recent advances in infrared (IR) thermography evaluation methods, there is a potential that indications of equipment's faults can be thermographically detected. However, many electrical devices are facing increasing challenges, which may compromise their safety and maintainability. Some of these problems, include aging and life process related issues. Additional threats are human-induced hazards or environmental incidents, which may destroy and destabilize safe operation of electrical installations. Industry has begun to distinguish that the combination of infrared (IR) thermography diagnostics methods and identification techniques, as well as additional inspection techniques, may play a significant part in retaining the functioning of process industry [1–4].

However, the analysis of the research in the above-mentioned area shows the number of reliable identification techniques in the IR thermographic inspection of electrical installations is still poor. Earlier studies conducted on electrical substation equipment and facilities, were based on the evaluation of maintenance operations [5]. Circuit breakers and power transformers were studied in [6]. The fault diagnosis approach described in [7, 8] is applied to the safety of single-phase induction motors including DC and synchronous motors. An intelligent clustering method that, which used an artificial neural network (ANN) to troubleshoot three-phase fuses and different connection faults, was proposed. Moreover, until today, researchers have been interested in the detection of anomalies existing on medium voltage electrical installations.

Infrared (IR) thermography is one of the most commonly used tools in electrical equipment inspection. One very important reason for its suitability is that most industrial electric plants are fairly unsafe to be tested during operating conditions, costly to switch in order to be monitored, or a combination of both.

Table 1. Arc flash protection distances

Operating voltage, V	Safety distance in feet
Less than 750	3
From 750 to 2000	4
From 2000 to 15000	16
From 15000 to 36000	19
More than 36000	Must be calculated

Table 2. IR imager characteristics

Thermo-vision (A 40M)	Solid state, microbolometer FPA sensor, 7.5 to 13 μm -40°C to $+2000^{\circ}\text{C}$ temperature difference band Solid object materials with emissivity: 0.1 to 0.95 For small separation, humidity is default value of 50% 50–55 images per second
-----------------------	---

Electric equipment seems to be convenient for IR thermography on a very basic level, since thermal energy is strongly correlated to electrical energy [9].

Infrared (IR) thermography evaluation of electric apparatus produces significant results exclusively if the device is in operating condition. In general, covers of the distribution cabinets need to be removed except the situations where appropriate IR lens is applied to permit the inspection of the equipment at a secure distance. When investigating electrical equipment in operation, special personal safety precautions should be retained to reduce the threat of arc flash. In addition, the surface temperature distribution could be compared above a wide region. Infrared (IR) thermography is an essential tool for detecting emerging faults before they turn into some kind of problematic faults. This technique can not only localize the failure of expensive component, but also supply detailed information on how to prevent burns, blasts and arc flashes in equipment. If the equipment is inspected properly within a correct period, it may personnel [10–12]. It is very important to distinguish between a point of heating due to a normal flow of electric current and a normal heating (transformer, relay, or contactor coil, etc.) characterized by the presence of faults. As long as results of IR thermographic inspection of electrical equipment can be saved in a digital form, a history of inspection results can be studied and evaluated in order to quantitatively identify equipment deterioration, which was appearing gradually.

The subsequent sections of this paper cover the following topics. Section 1 provides a description of the experimental setup and procedures used to inspect electrical equipment available in our laboratory. In Section 2 we present the thresholding methods used in this work which represent the main contribution of this research paper. Section 3 is dedicated to the presentation of the results obtained from the inspection of many processes and comparison of the performances of the thresholding methods used to detect the existing faults. Finally, Section 4 concludes the paper and gives recommendations for future work.

1. THERMOGRAPHIC MEASUREMENTS

The thermal radiometric imager has the ability of being exceptionally in small dimensions. It uses a 240×320 microbolometer FPA with a 24 mm Germanium lens providing a FOV (field of view) of $24^{\circ} \times 18^{\circ}$ with an essential focus separation of 30 cm. The spatial resolution is 1.3 mrad, thus indicates that at a separation of 1 m, one pixel represents a square of 1.3 mm \times 1.3 mm. Its thermal resolution at 20°C is 0.085°C . The sensitivity of radiometric sensor seemed to be convenient for the research undertaken since it operated in the 7.5–13 μm spectrum wavelength range. The connection between the IR camera and a personal computer (PC) can be realized using IEEE-1394 FireWire interface thus allowing a high rate of data transfer.

In order to perform a proper inspection (capture the best thermal image), it is recommended to follow the following guidelines [13, 14]:

- Confirm that the inspected component is running under no less than 40% of its charge. Low charges do not generate overheating, the accuracy of the efficiency measurement decreases as the load is reduced.

- Get closer to the equipment, and do not take measurements over barriers, particularly not over mirror. If the safety program permits, the electric-powered enclosure should be unclosed or a radiometric window must be used.
- Take into account the disturbing IR radiation sources. The objects with a lower emissivity reflect thermal radiation of other objects, including the Sun radiation. It may be interfaced along emitted object radiation with captured figure.

When inspecting a particular equipment, both the distance between the object and thermal imager has an important influence on the infrared thermography. For this reason, it has been chosen to place the IR imager at a distance of 2 m from a part to be inspected. When checking electrical equipment, it is usually recommended to set the emissivity value to 0.95. During the inspection, the ambient temperature near the equipment was about 20–25°C.

2. THERMAL DATA PROCESSING

There is no essential difference between methods of pre-processing of an IR image and a visible image. However, there is a need to improve quality of thermal images by removing some noise. The noise elimination technique was selected in accordance with a used IR inspection procedure and a type of the noise accompanying IR measurements. Generally, the noise as an influencing factor in IR radiation measurement methods can be represented by a Gaussian model [15].

2.1. ANN Approach

The use of artificial neural network (ANN) [16] enables the implementation of a feed-forward layered learning approach to neural system structure. The ANN process implements the back propagation procedure, which is standard in supervised training. It is possible to choose the number of layers to be used, and it is possible to select from a hyperbolic or logistic enabling function. Training is carried out by setting the values in the node in order to reduce the error between the output node's activation and the output. The difference is backpropagated across the model and the adaptation of the weights is performed recursively. So far, back propagation of the error algorithm using gradient descent is the most popular training technique when using ANNs.

The basic procedure for training a neural network (Fig. 1) is described as follows:

- (1) Initialize a set of weights for the network.
- (2) Add a value to the model and compute the related output data.
- (3) Check the actual results against the required results and compute the difference value.
- (4) Modify weights for all connections in the model.
- (5) Reiterate steps 2 through 4 with all the predefined input-output pairs until the error is decreased to a minimum value.

2.2. SVM Algorithm

The SVM algorithm was proposed by Vapnik [17–21]. SVM maps the input pattern into a kernel space where the patterns could be separated using an optimal hyperplane. The mapping is achieved through a kernel function (usually a non-linear function). Typical kernel functions are polynomial and Gaussian. The training of SVMs (Fig. 2) consists of finding the maximum margin hyperplane that maximizes the separation between two or more sets. The vectors that are at the maximum margin of the optimal hyperplane are called support vectors. SVM classifiers are completely characterized by support vectors, which greatly reduces their complexity and makes them less prone to over fitting issues [20]. Note that the sup-

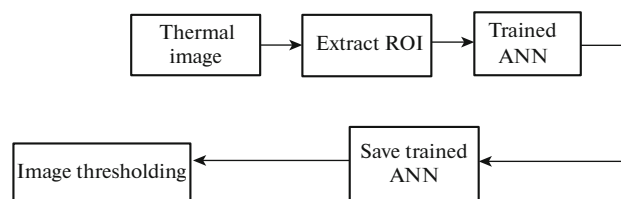


Fig. 1. Schematic representation of ANN approach for image binarization.

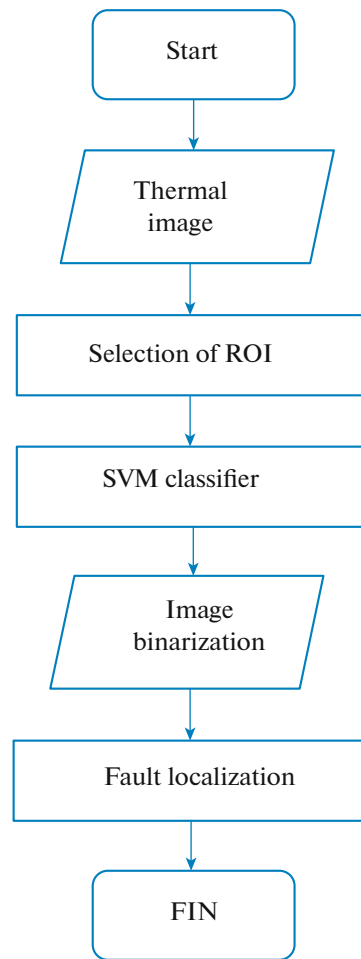


Fig. 2. Flowchart of SVM method.

port vector description formalism can be viewed as a generalized classifier with several other classifiers as special case. For example, if the kernel is chosen to be Gaussian, the SVM classifier created is essentially equivalent to be an RBF neural network. However, the difference is that the number of centers is automatically determined, and only the width of the Gaussian needs to be adjusted. Compared with traditionally trained RBF networks, this usually leads to better performance. The original SVM method proposed by Vapnik was a binary classification problem.

For training patterns $x_i \in \mathfrak{R}^n$, $i = 1 \dots n$ from a pair of sets, and a corresponding labels $y \in \mathfrak{R}^l$, thus y_i belongs to $\{-1, 1\}$, the linear function that separates the data set is defined by:

$$f(x) = wx + b, \quad (1)$$

where w and b are the parameters of the model. It is necessary to determine w and b that satisfy conditions (2) and (3):

$$f(x) = wx_+ + b, \quad (2)$$

where x_+ is the set of data belonging to the positive class. Furthermore:

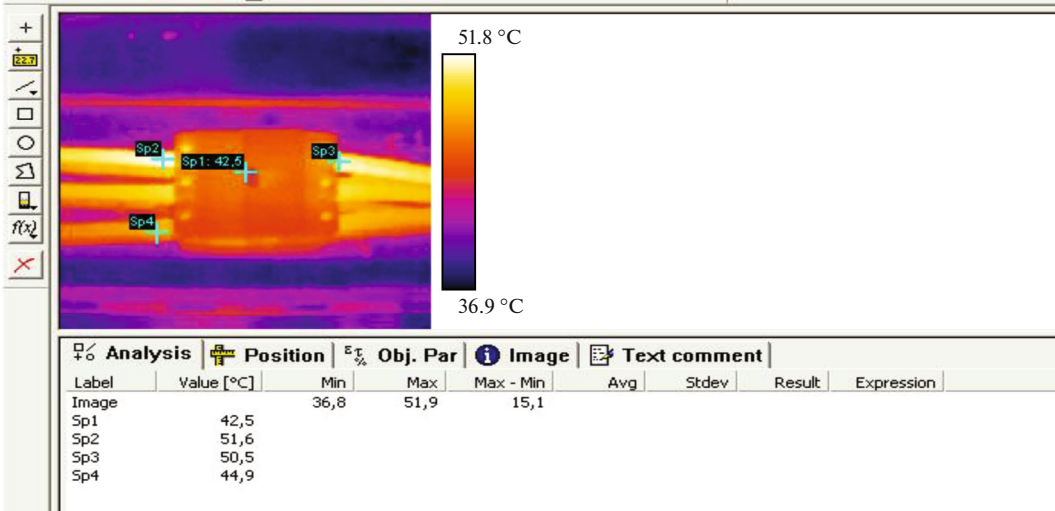
$$f(x) = wx_- + b, \quad (3)$$

where x_- represents the set of data belonging to the negative class.

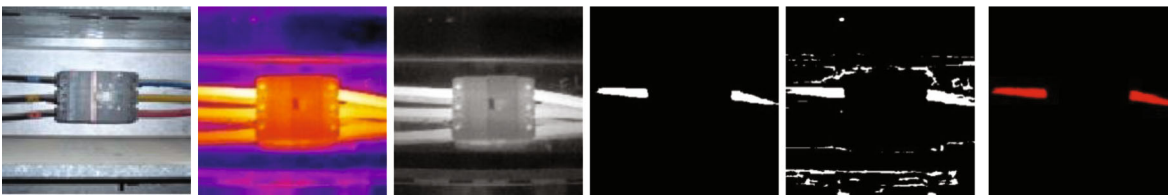
A linear separator can divide the data into two or more classes with the largest margin. Geometrically, we have:

$$x_+ = x_- + \delta w, \quad (4)$$

(a)



IR thermogram



Real image IR image Grey image SVM approach ANN approach Ground truth

Fig. 3. (a) Binarization methods used to identify electrical failure no. 1. (b) Binarization methods used to identify electrical failure no. 2. (c) Binarization methods used to identify electrical failure no. 3. (d) Binarization methods used to identify electrical failure no. 4.

where δ is the perpendicular distance between a data of the positive class and that of the negative class. By replacing x_+ from Eq. (3), in Eq. (1), and comparing with Eq. (2), we obtain the margin between these two classes:

$$\delta = \frac{2}{\|w\|^2}, \tag{5}$$

where δ is the perpendicular distance between a data from the positive class and that from the negative class.

Therefore, the hyperplane is optimal if only w is minimal. The optimization problem is expressed as:

$$\begin{cases} \min \frac{1}{2} \|w\|^2 \\ y_i(wx_i + b) \geq 1: \quad i \in \{1, \dots, n\}; \quad \forall x \in R^n. \end{cases} \tag{6}$$

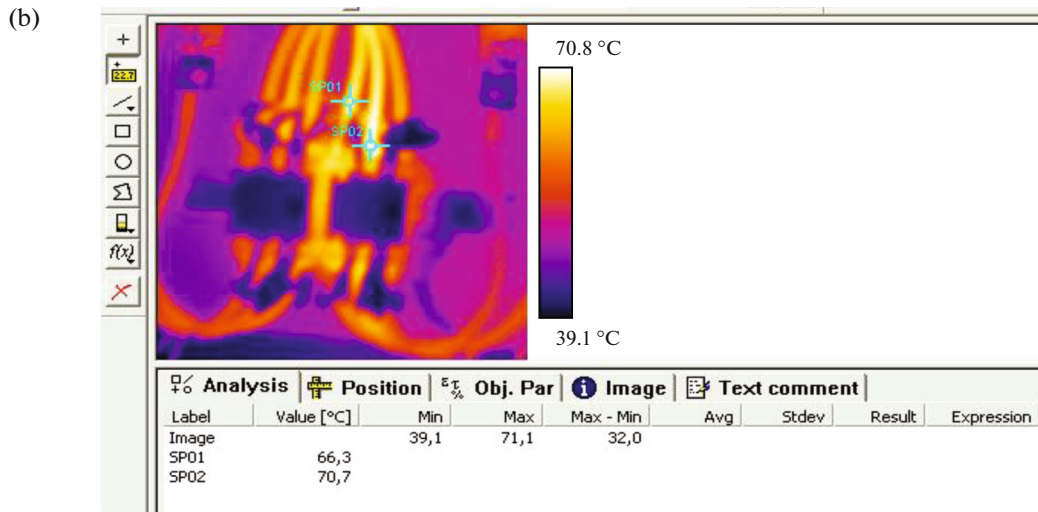
This leads to a determination of the margin δ , which is the largest if w is the smallest. As the optimization function is a quadratic function with linear constraints, the optimization problem is convex. The solution of the problem requires Lagrange multipliers. The new objective function becomes:

$$L_p = \frac{1}{2} \|w\|^2 - \sum_{i=1}^l \alpha_i y_i (x_i w_i + b) + \sum_{i=1}^l \alpha_i, \tag{7}$$

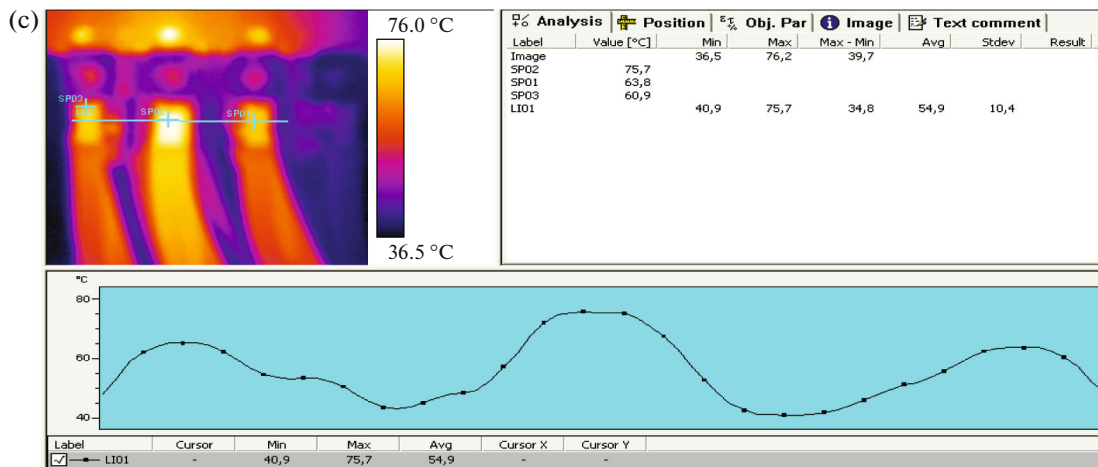
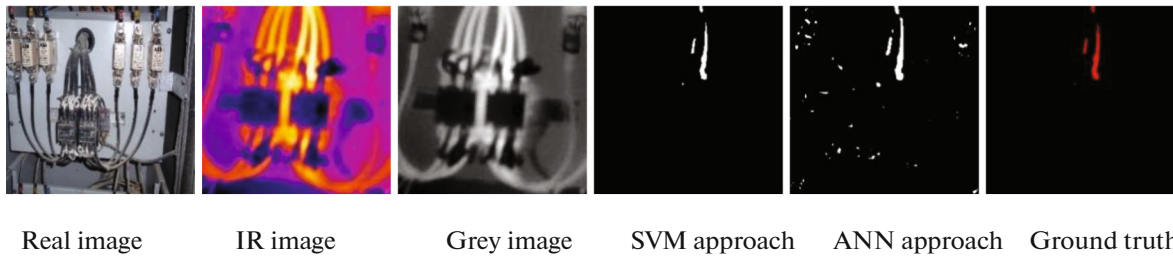
where α_i are the Lagrange multipliers.

The computing algorithms are as follows:

- (1) Prepare and filter the infrared data.



IR thermogram



IR thermogram

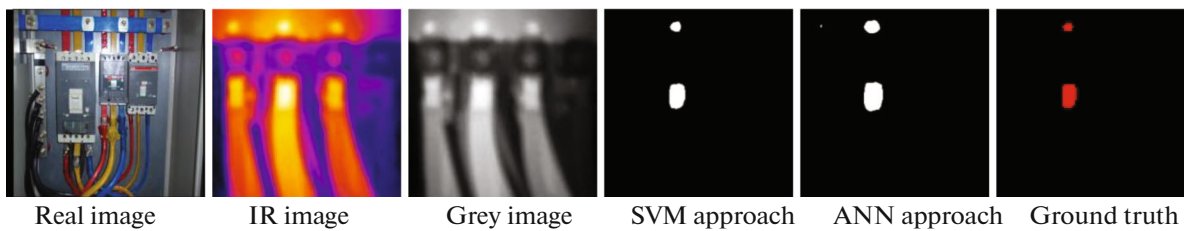
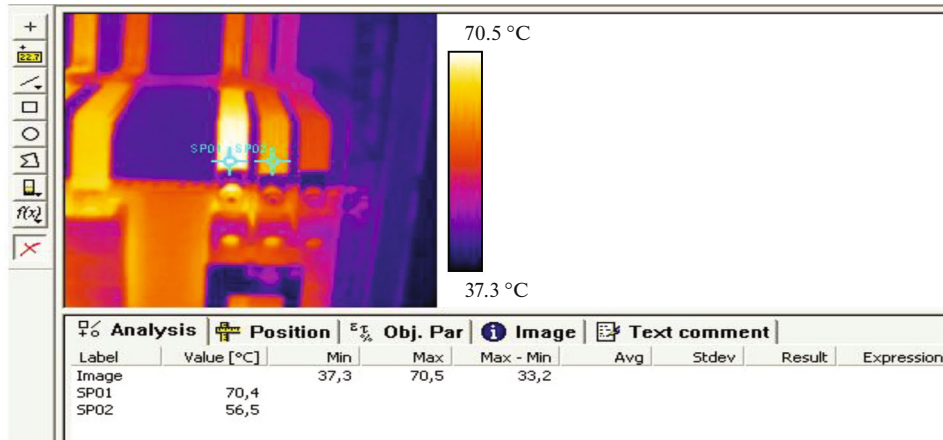


Fig. 3. (Contd.)

(d)



IR thermogram



Real image

IR image

Grey image

SVM approach

ANN approach

Ground truth

Fig. 3. (Contd.)

- (2) Select the ROI.
- (3) Choose the kernel function and train SVM classifier.
- (4) Use training data to train SVM classify for testing infrared thermography data.
- (5) inarize studied images.
- (6) Anomaly localization.

3. DATA ANALYSIS

In this section, we assess the performances of thresholding methods based on two supervised approaches. First, thermal images are obtained from the inspection of many plants using the A40 IR camera. With the aim of evaluating the quality of these approaches to detect equipment faults, comparisons were made between different classifiers, and four different images of actual electrical equipment collected from operating facilities. Images were segmented using different thresholding methods, namely, SVM and ANN approaches. The thresholded images show that the Trained SVM method produced better binarization efficiencies in comparison to the supervised ANN algorithm, and worked well for larger and smaller faults. It is worth mentioning that the use of the ANN requires more computational time due to the selection of training and verification of Regions of Interests. In terms of images, infrared thermography binarization produces higher accuracy. This is because the IR thermography image contains less variability in the electrical image, and at the same time increases the visibility of the failures, otherwise these faults cannot be detected even in a real image. Concerning the first result (Fig. 3a), and comparing it with other cables, it was noticed that cable 1 is heated as shown in Spot 2 (51.6°C). The thermal energy emitted by a cable is related to the square of the current flowing through it. A small increase in the line current will cause a significant increase in the temperature, so it is recommended to check the circuit breaker connection. The second image shows that the contactor cable is heated as shown on spot SP01 (70.7°C). The hot spots are clearly visible in the thermal image. The temperature signal increase indicates a serious problem in the joints. Therefore, the contactors, resistors, cables, and capacitors need to be checked. In the third

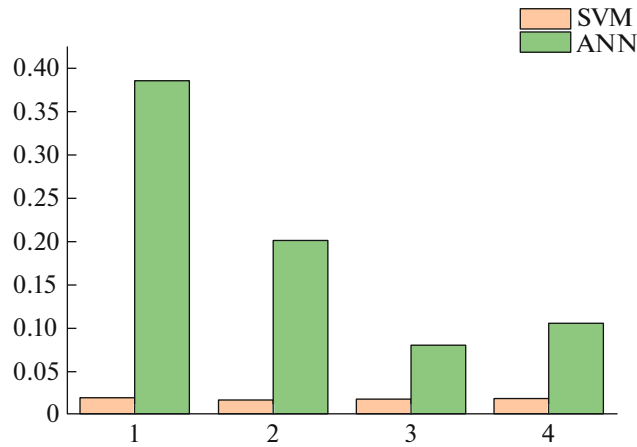


Fig. 4. Binarization ME of SVM and ANN.

case, it was noted that cable 2 is heated; this is caused by an excess of charge or a disconnected tightening. In this case, it is recommended to clean and tight all joints and to verify the load in the circuit. The image from the last inspection shows that cable 1 is heated (Sp01 indicates a temperature of 70.4°C), which comes from the circuit breaker. Therefore, it is advised to tightly connect and test the circuit breaker.

In this section, two criteria for binarization evaluation, namely, the misclassification error (ME) and the relative foreground area error, were used, as defined in [3]. The ME parameter is used to measure the percentage of background pixels misclassified as foreground, and inversely. It can be represented as:

$$ME = 1 - \frac{|B_{0Id} \cap B_{0k}| + |B_{1Id} \cap B_{1k}|}{|B_{0Id}| + |B_{1Id}|}. \quad (8)$$

The B_{0Id} and B_{1Id} parameters indicate the non-faulty and faulty pixels of the reference image, individually, B_{0k} then B_{1k} represent the non-faulty pixels plus faulty pixels of the binarized image, respectively, and $|\cdot|$ represents the unit set. The ME varies from zero for a well-binarized data to one unity for a fully imperfectly thresholded data.

The critical assessment index for the support vector machine and ANN approaches is displayed in Fig. 4. The baseline image uses a reference image to compare the threshold results. Figure 3 shows the binarization results of the four faults. For all the results, the misclassification error of the support vector machine method is smaller than that of the artificial neural network method. For the SVM method, the mean of non-classified pixel difference is 1.80%, and for ANN approach, the average pixel misclassification error is 19.30%.

3.1. Metrics Evaluation

Pixel-level performance was evaluated using three metrics taking into account only the global amount of intersecting pixels of estimation and ground truth, total amount of predicting pixels and total amount of ground truth pixels.

The E parameter below denotes the predictable pixels created by the fault detection approach, while V refers to the pixels located in Ground truth images.

$$\text{precision} = \frac{E \cap V}{E}, \quad (9)$$

$$\text{recall} = \frac{E \cap V}{V}, \quad (10)$$

$$F_{\text{measure}} = 2 \times \frac{\text{precision} \times \text{recall}}{\text{precision} + \text{recall}}. \quad (11)$$

A higher level of satisfaction is guaranteed by a better value of F-measure.

Table 3. Pixel level evaluation in thermal data by using three metrics

Pixel level evaluation	Thresholding approaches	
	SVM	ANN
Recall	98.52	92.64
Precision	96.89	93.08
F-measure	98.45	92.81

The SVM method provides the highest results using F-measure, which includes harmonic mean of precision and recall. Pixel level evaluation confirms that this approach is better than the ANN thresholding algorithm in terms of recall, accuracy, and F-measure (Table 3).

4. CONCLUSIONS

The image processing method used in this study deals with some industrial case anomalies, which were obtained from inspections of electrical equipment operating at some industrial plants. Infrared thermography inspection of electrical equipment can locate many types of failures, and seems to be very effective in terms of cost and time. The results and discussion involved here show that the SVM processing technique can detect all electrical faults hidden in IR images. The SVM classifier provides very high accuracy (96.89%) and F-measure (98.45%), thus proving that the SVM method can accurately detect a major part of the pixels reflecting a fault. Consequently, the suggested approach can be on a frequent base, thus helping to prevent failures and plan repairs in advance. As a future work, we plan to use IR thermographic diagnostics to check the quality of steel products.

REFERENCES

- Hui, Z. and Fuzhen, H., An intelligent fault diagnostics method for electrical equipment using infrared images, *Proc. 34th Chin. Control Conf.*, Hangzhou, 2015, pp. 6372–6376.
- Laib dit Leksir, Y., Bouhouche, S., Boucherit, M.S., and Bast, J., Adaptive support vector machine—based surface quality evaluation and temperature monitoring, *Int. J. Adv. Manuf. Technol.*, 2012, vol. 67, nos. 9–12, pp. 2063–2073.
- Laib dit Leksir, Y., Mansour, M., and Moussaoui, A., Localization of thermal anomalies in electrical equipment using Infrared thermography and support vector machine, *Infrared Phys. & Technol.*, 2018, vol. 89, pp. 120–128.
- Glowacz, A., Fault diagnosis of electric impact drills using thermal imaging, *Measurement*, 2021, vol. 171, p. 108815.
- Pedro, J., Zarco Perinán, J., and Ramos, L.M., A novel method to correct temperature problems revealed by infrared thermography in electrical substation, *Infrared Phys. & Technol.*, 2021, vol. 113, p. 103623.
- Jadin, M.S., Taib, S., and Ghazali, K.H., Feature extraction and classification for detecting the thermal faults in electrical installations, *Measurement*, 2014, vol. 57, pp. 15–24.
- Glowacz, A. and Glowacz, Z., Diagnosis of the three-phase induction motor using thermal imaging, *Infrared Phys. & Technol.*, 2017, vol. 81, pp. 7–16.
- Singh, G. and Naikan, V.N.A., Infrared thermography based diagnostics of inter-turn fault and cooling system failure in three-phase induction motor, *Infrared Phys. & Technol.*, 2017, vol. 87, pp. 134–138.
- Vollmer, M. and Möllmann, K.P., *Infrared Thermal Imaging: Fundamentals, Research and Applications*, Hoboken: Wiley, 2010.
- Stauffer, B. and Traister, J., *Electrician's Trouble Shooting and Testing Pocket Guide*, New York: McGraw-Hill, 2007.
- David, L.P. and Jose, A.D., Application of Infrared Thermography to Failure Detection in Industrial Induction Motors: Case Stories, *IEEE Trans. Ind. Appl.*, 2017, vol. 53, no. 3, pp. 1901–1908.
- Vavilov, V. and Burleigh, D., *Infrared Thermography and Thermal Nondestructive Testing*, Berlin: Springer Nature, 2019.
- Flir systems AB, User's manual FLIR Thermacam Researcher ver 2.9, 1997–2007.
- Maldague, X.P.V., *Theory and Practice of Infrared Technology for Nondestructive Testing*, New York: Wiley, 2001.

15. Shaikh, S.H., Maiti, A.K., and Chaki, N., A new image binarization method using iterative partitioning, *Mach. Vision Appl.*, 2013, vol. 24, pp. 337–350.
<https://doi.org/10.1007/s00138-011-0402-4>
16. Zhao, H., Zheng, J., Wang, Y., Yuan, X., and Li, Y., Portrait style transfer using deep convolutional neural networks and facial segmentation, *Comput. & Electr. Eng.*, 2020, vol. 85, article ID 106655.
<https://doi.org/10.1016/j.compeleceng.2020.106655>
17. Wun, Z., Zhang, H., and Liu, J., A fuzzy support vector machine algorithm for classification based on a novel PIM fuzzy clustering method, *Neurocomputing*, 2014, vol. 125, pp. 119–124.
18. Wu, J., Lou, J., Wang, Y., and Li, M., Infrared Image Segmentation for Power Equipment Failure Based on Fuzzy Clustering and Wavelet Decomposition, *Int. Conf. Comput. Intell. Commun. Networks*, Jabalpur, 2015, pp. 1274–1277.
19. Hui, Z. and Fuzhen, H., A novel intelligent fault diagnosis method for electrical equipment using infrared thermography, *Infrared Phys. & Technol.*, 2015, vol. 73, pp. 29–35.
20. Langone, R., Alzate, C., Ketelaere, B.D., Vlasselaer, J., Meert, W., and Suykens, A.K., LS-SVM based spectral clustering and regression for predicting maintenance of industrial machines, *Eng. Appl. Artif. Intell.*, 2015, vol. 37, pp. 268–278.
21. Duda, R., Hart, P., and Stork, D., *Pattern Classification*, New York: Wiley-Interscience, 2001.